Heat Transfer Engineering

ISSN: (Print) (Online) Journal homepage: https://www.tandfonline.com/loi/uhte20

Experiments and Correlations for Single-Phase Convective Heat Transfer in Brazed Plate Heat Exchangers

Angela Mutumba, Francesco Coletti, Alex Reip, Mohamed M. Mahmoud & Tassos G. Karayiannis

To cite this article: Angela Mutumba, Francesco Coletti, Alex Reip, Mohamed M. Mahmoud & Tassos G. Karayiannis (2023) Experiments and Correlations for Single-Phase Convective Heat Transfer in Brazed Plate Heat Exchangers, Heat Transfer Engineering, 44:3, 211-231, DOI: 10.1080/01457632.2022.2049539

To link to this article: https://doi.org/10.1080/01457632.2022.2049539

Published online: 17 Mar 2022.

HEAT TRANSFER ENGINEERING
2023, VOL. 44, NO. 3, 211–231
https://doi.org/10.1080/01457632.2022.2049539

Taylor & Francis
Taylor & Francis Group

Experiments and Correlations for Single-Phase Convective Heat Transfer in Brazed Plate Heat Exchangers

Angela Mutumba[a], Francesco Coletti[b], Alex Reip[c], Mohamed M. Mahmoud[a,d], and Tassos G. Karayiannis[a]

[a]Department of Mechanical and Aerospace Engineering, Brunel University London, Uxbridge, Middlesex, UK; [b]Department of Chemical Engineering, Brunel University London, Uxbridge, Middlesex, UK; [c]Oxford NanoSystems, Abingdon Business Park, Oxford, UK; [d]Faculty of Engineering, Zagazig University, Zagazig, Egypt

ABSTRACT

This study presents the single-phase heat transfer and pressure drop characteristics of R1233zd(e) in a Brazed Plate Heat Exchanger (BPHE). Experiments on single-phase, water-to-water, were initially conducted and a correlation for the convective heat transfer coefficient of the hot water side was derived by applying the modified Wilson plot method. The experiments covered a range of Reynolds number from 80 to 1600 and Prandtl number from 2.8 to 7.0. Subsequent experiments were conducted with water-to-R1233zd(e) covering a refrigerant range of Reynolds number from 700 to 1450 and Prandtl number from 4.5 to 4.9. The results were used to assess existing correlations in the literature predicting the Nusselt number and Fanning friction factor in BPHEs. Finally, new correlations for both the hot (water) and cold (refrigerant) sides are proposed for single-phase heat transfer for this geometry covering the conditions above. The proposed refrigerant heat transfer correlation predicted 97% of all data within the ± 10% error bands at a mean absolute error value of 5.7%.

Introduction

Plate Heat Exchangers (PHEs) have been used successfully in several industries such as oil and gas, refrigeration, and energy generation systems, due to their high surface area to volume ratio. They are particularly beneficial to the refrigeration industry because the corrugated plate surfaces and small hydraulic diameter promote turbulence in the flow channels. Such flow (swirl or vortex flow), as well as the disruption and reattachment of the boundary layer contribute to enhanced heat transfer rates [1]. Consequently, they provide an enhanced thermal-hydraulic performance with an added feature of miniaturization compared to the traditional shell and tube heat exchangers.

A literature survey shows that there has been a lot of experimental work on Plate Heat Exchangers (PHEs) focused on refrigerant applications. Common working fluids included the use of both pure fluids and mixtures. However, the use of such substances was found to affect the ozone layer and contributed to greenhouse effects. Consequently, international environmental regulations promoted the development of alternative and suitable refrigerants such as Hydrofluoroolefins (HFOs) with both low Global Warming Potential (GWP) and Ozone Depletion Potential (ODP). However, their performance in energy conversion systems such as the Organic Rankine Cycles (ORCs) is yet to be determined. ORCs are particularly well-suited to converting low- to medium-grade heat (below 100 °C to 300-400 °C) to power. Recently, HFOs like R1233zd(e) and R1336mzz(z) have shown to be a promising replacement for R245fa; commonly used in ORCs. For example, Moles et al. [2] evaluated the performance of R1233zd(e) and R1336mzz(z) as potential substitutes for R245fa in an ORC for waste heat recovery. Throughout the range of operating conditions and configurations examined, the alternative refrigerants consumed lower pumping power and could therefore achieve higher values of net cycle efficiency. This study showed that R1233zd(e) required 10.3%−17.3% less pumping power and produced up to 10.6% higher net cycle efficiencies than R245fa, over the range of cycle conditions examined. The possibility of replacing R245fa

CONTACT Professor Tassos G. Karayiannis tassos.karayiannis@brunel.ac.uk Department of Mechanical and Aerospace Engineering, Brunel University London, Uxbridge, Middlesex UB8 3PH, UK

Nomenclature

A_{ch}	flow area, [m^2]
A_{eff}	effective heat transfer area, [m^2]
A_p	projected heat transfer area, [m^2]
b	corrugation amplitude or plates spacing, [m]
b_i	systematic error
BPHE	Brazed Plate Heat Exchangers
C_p	specific heat, [J/kg K]
C_1, C_2, C_3	empirical constants in Eq. (8)
D_e	equivalent diameter, [m]
D_h	hydraulic diameter, [m], $(D_h = 2b)$
D_p	port diameter, [m]
EES	Engineering Equation Solver
f	Fanning friction factor
g	gravitational constant, [m/s^2]
G	mass flux, [kg/m^2 s]
GPHE	Gasket Plate Heat Exchangers
GWP	Global Warming Potential
h	heat transfer coefficient, [W/m^2 K]
HFOs	Hydrofluoroolefins
k	thermal conductivity, [W/m K]
L	characteristic length, [m]
L_{eff}	core length, [m]
L_h	plate length, [m]
L_p	port to port plate length, [m]
m	mass flow rate, [kg/s]
MAE	Mean Absolute Error
N	number of plates
N_{ch}	number of channels
n_p	number of passes on the given fluid side
N_p	effective number of plates
Nu	Nusselt number, $(Nu = hD_h/k)$
ODP	Ozone Depletion Potential
ORC	Organic Rankine Cycle
P	pressure, [Pa]
ΔP	pressure drop, [Pa]
Pr	Prandtl number, $(\mathrm{Pr} = C_p\mu/k)$
PHE	Plate Heat Exchanger
Q	heat transfer rate, [W]
R	thermal resistance, [K/W]
R^2	coefficient of multiple determination in regression analysis
Re	Reynolds number, $(Re = GD_h/\mu)$
s_x	standard deviation
t	plate thickness, [m]
T	temperature, [K]
ΔT	temperature difference, [K]
ΔT_{ln}	log-mean temperature difference, [K]
U	overall heat transfer coefficient, [W/m^2 K]
UA	overall thermal conductance, [W/K]
W	plate width, [m]
X	parameter defined in Eq. (2)
Y	Arbitrary variable in Eq. (17)

Greek symbols

β	Corrugation/chevron angle, [degree]
ϵ	uncertainty
γ	aspect ratio
λ	corrugation pitch, [m]
μ	dynamic viscosity, [Pa.s]
ρ	density, [kg/m^3]
ϕ	surface enlargement factor, (A_{eff}/A_p)

Subscripts

a	acceleration
c	cold
cal	calculated
exp	experiment
f	frictional
g	gravitational
h	hot
i	inlet
m	mean
o	outlet
p	port
pt	plate
r	refrigerant
sat	saturation
tt	total
w	water

with R1233zd(e) is also supported by the similar thermo-physical properties as shown in Table 1. The values reported in Table 1 are based on Engineering Equation Solver (EES) software and reference [3].

There are several types of PHEs but the most widely used is the chevron/herringbone pattern with over 60 different patterns from various manufactures [4]. These are further categorized into gasketed and brazed PHEs. The traditional Gasketed Plate Heat Exchangers (GPHEs) consist of thin rectangular pressed metal plates assembled between bordering gaskets and clamped together in a frame. Brazed Plate Heat Exchangers (BPHEs) were later developed to resolve some of the inherent limitations of the GPHEs, by eliminating the need for frames or gaskets that were susceptible to leaks. The stainless-steel plates are brazed together using a brazing material such as copper, making them able to operate at higher pressures and temperatures. More recently, extensive work [5–7] has been done to improve the performance of PHEs through design optimization and numerical investigation. Although there have been numerous publications on heat transfer and pressure drop in GPHEs, there is less work on BPHEs.

A number of studies [8–25] that investigated the single-phase heat transfer and pressure drop in BPHEs and some GPHEs, from 1981 to 2017, are included in Table A1 in Appendix A. A total of 28 heat transfer correlations for GPHEs were summarized by Ayub [26], in which most correlations adopted the form of the Dittus Boelter equation [27] for the convective heat transfer coefficient in tubes.

Table 1. Thermo-physical properties of R245fa and low GWP alternative R1233zd(e) based on EES software and values with * are taken from [3].

Parameters	R245fa	R1233zd(e)
ODP	0*	0.00034*
GWP	1030*	1-7*
Boling point (°C)	14.08	17.97
Saturation pressure (bar) at 300 K	1.59	1.38
Liquid specific heat (kJ/kg K) at 300 K	1.33	1.25
Liquid density (kg/m^3) at 300 K	1333.5	1258.3
Enthalpy of vaporization (kJ/kg) at 300 K	189.2	190.8
Flammability	Non-flammable*	Non-flammable*
Molecular mass (kg/kmol)	134	130.5
Critical Pressure (bar)	36.5	35.7
Critical Temperature (°C)	154.01	165.6

For single-phase flow, studies have shown that the geometric parameters such as the chevron angle (β), hydraulic (D_h) or equivalent diameter (D_e), corrugation pitch (λ) and enlargement factor (ϕ), have a strong influence on the thermal and hydraulic performance of the heat exchanger. Of all the parameters that define the geometry of the plates, the chevron angle is perhaps the most affecting parameter. It is widely recognized that both heat transfer and pressure drop increase with higher chevron angles [10]. However, the improved heat transfer comes at a higher pressure drop penalty and the increase in the friction factor with mass flow rate is quicker than that of the heat transfer coefficient [28]. The correlations found in open literature are therefore limited and only applicable to the geometry and operating conditions stated in the study, because of the large number of geometric parameters that can affect the fluid flow and heat transfer. However, despite the influence of the geometry, details of the geometric parameters are seldom reported due to propriety nature of each plate design. For example, Palmer et al. [15] measured the two-phase heat transfer coefficient for R22, R290, R290/600a, and R32/152a in a BPHE, but the study did not report values of the corrugation angle, pitch, enlargement factor and the range for which their proposed correlations were valid. Additionally, there is lack of consistent definition of these geometrical parameters. In particular, the hydraulic diameter, plate length and the heat transfer area used to evaluate the heat transfer coefficient and friction factor, which would have a significant impact on the results. Therefore, to have a reliable comparison of these correlations, the differences in these definitions need to be accounted for.

Single-phase heat transfer studies are important both on their own right, but also as a means to arrive at relations for two-phase flow in BPHEs. In two-phase flow applications, the correlations used, may include an element of single-phase heat transfer during sub-cooled boiling, i.e. before boiling commences, as reported by Hsieh and Lin [29]. Therefore, a comprehensive analysis and understanding of the single-phase heat transfer process in BPHEs is required. Furthermore, most single-phase correlations are reported for water-to-water configurations for which it was often found that the Nusselt number correlation for the hot and cold side was the same. Hayes and Jokar [8] conducted experiments with hot water and chilled dynalene and demonstrated that it is essential to report correlations for the hot side and cold side when using two different fluids.

Despite the more recent published correlations, the conclusion that there is still no agreement between correlations for the prediction of the heat transfer coefficient in BPHEs is still valid. Kim and Park [12] conducted a study using water and two different BPHEs with the same corrugation angle $(\beta = 65^\circ)$, but all other parameters were different. In comparing their results with correlations in literature, it was reported that the friction factor was mostly under-predicted by correlations developed for GPHEs. They attributed this to the additional flow restriction due to the brazing points, which resulted in a higher pressure drop. Other past correlations used in their comparison that over-predicted the friction factor were developed for a higher range of Reynolds number and a different plate pattern. Their data showed an increase in the pressure drop with a reduced hydraulic diameter in agreement with Faizal and Ahmed [30]. The enlargement factor was found to affect the heat transfer rates and as a result, it was included in the proposed correlation for the friction factor and Nusselt number.

Yang et al. [24] investigated the single-phase heat transfer for nine BPHEs with different geometric parameters using an ethylene glycol - water mixture (65 vol %) for which properties were taken at $0\,^\circ\text{C} - 35\,^\circ\text{C}$. Using just their experimental data, the authors developed a correlation for the heat transfer coefficient for a limited range of Reynolds number ($50 < \text{Re} < 500$) and Prandtl number ($50 < \text{Pr} < 150$). The comparison with others showed poor agreement, which was attributed to the geometrical variation. This led the authors to develop a more generalized correlation using an experimental data base from 22 different GPHEs (including their own) and 25 correlations found in literature. This correlation covered a wide range of geometric parameters and working conditions, i.e., $50 < \text{Re} < 8000$; $2 < \text{Pr} < 290$; $27^\circ < \beta < 63^\circ$; $1.16 < \phi < 1.464$; $0.557 < \gamma < 1.290$.

However, the authors did not specify the fluids used in this data set or identify the 25 empirical correlations. Furthermore, the correlation demonstrated a poor prediction accuracy of ± 50% for 95% of the data. The possible number of combinations of geometric parameters is very large therefore, most research has focused on qualitative performance instead of searching for a universal correlation for the single-phase heat transfer in PHEs.

As mentioned above, there is still lack of cohesive design information available in the open literature due to the proprietary nature of the industry. The brazed points in BPHEs introduce an additional structure in the flow channels, which reduces the contact thermal resistance and enhances turbulence. Therefore, with the introduction of new low GWP and ODP refrigerants and the different thermal-hydraulic characteristics of BPHEs compared to GPHEs, there is a need for the development of new heat transfer and pressure drop correlations. Our literature review revealed that there is only limited work reported on flow boiling heat transfer performance of new low-pressure refrigerants like R1233zd(e) in BPHEs that could be used in energy conversion systems, [15, 16] and even less so on the single-phase pressure drop and heat transfer rates. Hence, there is a need for further research in this area.

In the present study we investigate single-phase heat transfer rates and pressure drop for a water-R1233zd(e) in a BPHE. On the water side, the Reynolds number ranged from 80 to 1600 and a Prandtl number from 2.8 to 7.0. The range of Reynolds number and Prandtl number on the R1233zd(e) side was from 700 to 1450 and 4.5 to 4.9, respectively. The fluid properties for these dimensionless numbers for the water and refrigerant were taken at the mean temperature (average of inlet and outlet) for the water and the refrigerant side. For the water side the mean temperature ranged from 18 °C to 63 °C and for the refrigerant side from 15 °C to 25 °C. This is in agreement with the process used in [10, 31]. Our results were compared with existing correlations and agreements and deviations were pointed out. A new correlation predicting the heat transfer coefficient for the hot water side plus one for the refrigerant side was developed and recommended.

Experimental facility

Experimental flow loop

A schematic of the experimental facility is shown in Figure 1 where the tested BPHE has a 1-1 single pass flow arrangement ($n_p = 1$) and is set up in a counter

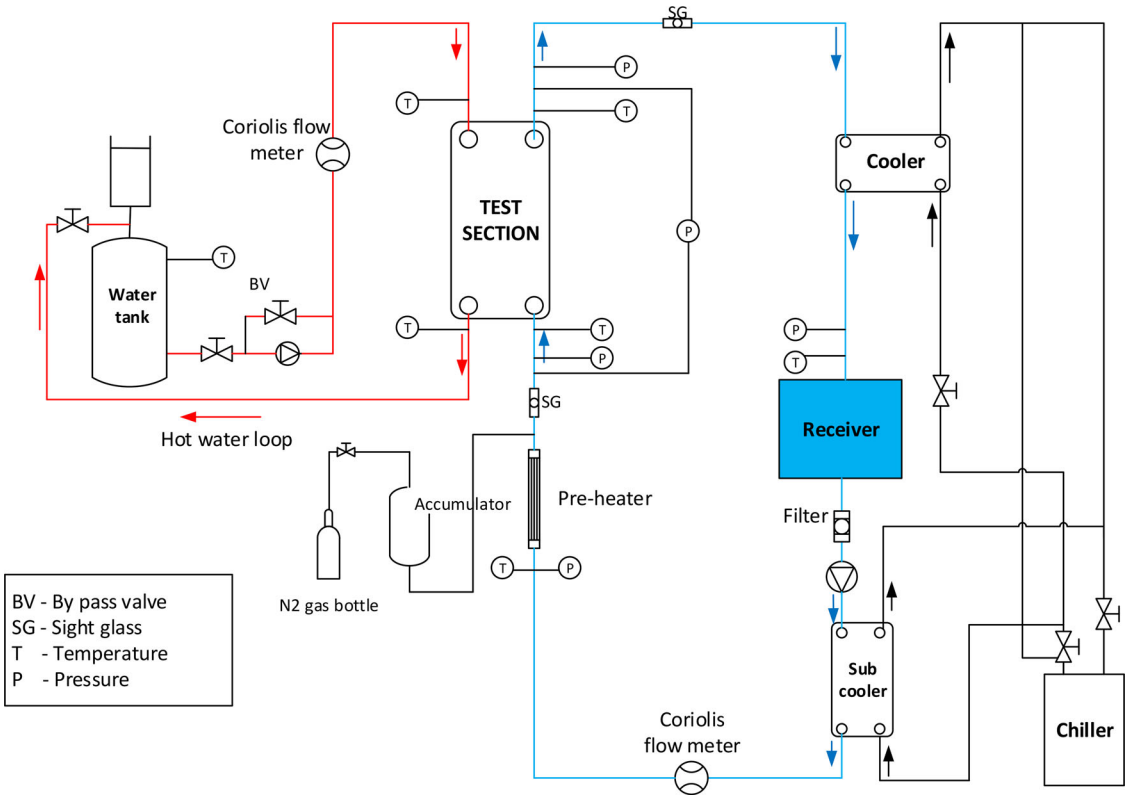

Figure 1. Schematic of the experimental facility.

flow direction. The set up consists of three loops, namely: the hot water, the refrigerant and the cold-water loop. The refrigerant loop consists of a receiver, a gear pump (DGS.99EEET2NM from Tuthill®), a Coriolis mass flowmeter (OPTIMASS 3400 C S04 for mass fluxes up to 0.125 kg/s from Krohne), a tube pre-heater, the BPHE test section and a BPHE cooler and subcooler. The refrigerant is pumped by a variable frequency gear pump from the receiver to the sub-cooler to the pre-heater, where it can be heated to achieve the desired temperature at the inlet of the test section. The refrigerant then goes through the tested BPHE where it is heated and returned to the cooler and the receiver. A bladder accumulator connected to a nitrogen cylinder and a pressure regulator is used to control and damp any pressure fluctuations in this loop. The cold-water loop is able to supply a propylene glycol water mixture at temperature ranging between 8 and 35° C with a stability within ± 0.1 K to feed the sub-cooler and the cooler. The hot water loop supplies water from a 117 L tank (heated by a 3 kW variable electric heater) at a temperature range of $20-80\,^{\circ}C$ to feed the test section BPHE. The water mass flow rate is measured by a Coriolis mass flowmeter (OPTIMASS 7400 C S10 for mass fluxes up to 0.3 kg/s from Krohne) and pumped to the test section. The refrigerant and water temperatures at the inlet and outlet of the tested BPHE are measured by T-type thermocouples. The refrigerant pressure at the inlet and outlet of the tested BPHE are measured by two pressure transducers (PXM319-010GI), whilst the refrigerant pressure drop is measured by a differential pressure transducer (PX2300-5DI). All measurements are recorded by a data logger (Picolog 6) linked to a PC. The thermophysical properties of water and R1233zd(e) were obtained from EES software.

Test brazed plate heat exchanger

Figure 2 depicts the schematic diagram of the BPHE used in the experiment with the geometric parameters detailed in Table 2. All the geometric parameters of the tested unit were doubly confirmed, in addition to the manufacturer-supplied information. The stainless-steel BPHE consists of 12 plates and is installed in a vertical position, with the refrigerant flowing upwards against gravity. The hot water enters at the top and leaves at the bottom of the heat exchanger.

Establishing the definition of the geometries of the plates is crucial to the accurate analysis of the heat transfer and pressure drop in BPHEs. For example, calculating the flow hydraulic diameter in the channels corresponds to the flow velocity and in turn can characterize the Reynolds number, which is used in the correlation of the Nusselt number and friction factor.

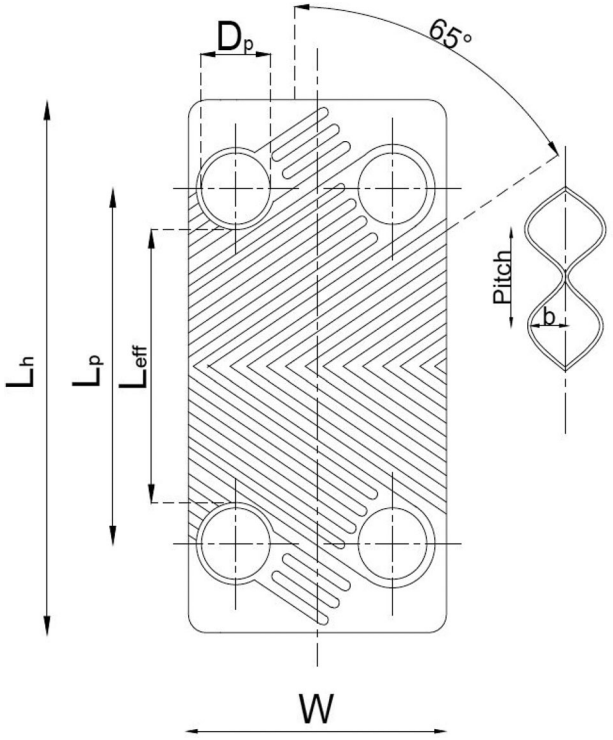

Figure 2. Schematic of one of the plates of the tested BPHE.

Table 2. Geometry of the tested BPHE.

Port-to-port length	$L_p = 278.5$ mm
Plate length	$L_h = 296.2$ mm
Core length	$L_{eff} = 260.\ 8$ mm
Plate width	$W = 71.3$ mm
Projected area of single plate	$A_p = 0.0186\ m^2$
Effective area of single plate	$A_{eff} = 0.0225\ m^2$
Total effective heat transfer area	$A_{eff} \times N_p = 0.225\ m^2$
Corrugation angle	$\beta = 65^{\circ}$
Corrugation amplitude	$b = 2.17$ mm
Surface enlargement factor	$\phi = 1.21$
Hydraulic diameter	$D_h = 2b = 4.34$ mm
Corrugation pitch	$\lambda = 6$ mm
Plate thickness	$t = 0.3$ mm
Aspect ratio	$\gamma = \frac{2b}{\lambda} = 0.72$
Number of plates	$N = 12$
Effective number of plates	$N_p = 10$
Number of channels	$N_{ch} = N_p - 1 = 11$
Channels on refrigerant side	$N_{ch,r} = 5$
Channels on hot-water side	$N_{ch,w} = 6$
Port diameter	$D_p = 0.01675$ m
Thermal conductivity of plate (stainless steel at 25 °C)	$k_{pt} = 13.4$ (W/m.K)
Single channel flow area	$A_{ch} = bW = 1.55 \times 10^{-4}\ m^2$

In this paper the hydraulic diameter is defined as:

$$D_h = 2b \tag{1}$$

The corrugations increase the surface area of the plate compared to a flat plate. The surface enlargement factor (ϕ) is a ratio used to express the

increased area as specified by the manufacturer. ϕ for a sinusoidal corrugated plate surface is a function of the corrugation pitch (λ), and mean spacing between the plates (b), as follows, [32]:

$$\phi \approx \frac{1}{6}\left(1+\sqrt{1+X^2}+4\sqrt{1+\frac{X^2}{2}}\right)=\frac{A_{eff}}{A_p} \quad (2)$$

where $X=\frac{\pi b}{\lambda}$ and the projected area (A_p), as if there were no corrugations, can be approximated by Eq. (3):

$$A_p = L_{eff} W \quad (3)$$

where $L_{eff}=L_p-D_p$ in accordance with [32]. It is difficult to accurately determine the effective area (A_{eff}), due to the corrugated surface and therefore it is often expressed as [5]: $A_{eff}=A_p\phi$.

It should be noted that the corrugation pattern is not always perfectly sinusoidal, and therefore several manufactures may specify the enlargement factor for their own atypically shaped surfaces. Typical values range between $1.1-1.4$, which indicates an increment in theheat transfer area of up to 40% due to the corrugated plate surface.

Published summaries [26, 33] of correlations in literature show that there are different definitions of the heat transfer area and the hydraulic diameter, and a comparison of experimental data can only be valid with identical definition of parameters. The projected heat transfer area (A_p) as opposed to the effective area (A_{eff}) is used to evaluate the overall heat transfer coefficient (U-value) and to calculate the minimum heat transfer coefficient in accordance with Longo and Gasparella [16], Longo et al. [17], and Longo [34]. So existing correlations that regard A_{eff} as the heat transfer area require modification and similarly so do correlations with $D_h={}^{2b}/_{\phi}$. Table A1 in Appendix A clearly specifies the diameter and the surface area used by the different researchers. In the comparisons that follow with the present results, the equations given were converted to the hydraulic diameter $D_h=2b$ and the projected area (A_p) used in this study as shown in Appendix B.

Data reduction

Heat transfer

The overall heat transfer coefficient is derived from the ratio of the heat load Q, to the total projected heat transfer area of a single plate A_p multiplied by N_p and the logarithmic mean temperature ΔT_{ln} as suggested by Shah and Focke [32]:

$$U=\frac{Q}{N_p A_p \Delta T_{ln}} \quad (4)$$

where the logarithmic mean temperature difference is given by:

$$\Delta T_{ln}=\frac{(T_{h,o}-T_{c,i})-(T_{h,i}-T_{c,o})}{\ln\frac{(T_{h,o}-T_{c,i})}{(T_{h,i}-T_{c,o})}} \quad (5)$$

The logarithmic mean temperature difference approach was used, based on the assumption of a constant heat transfer coefficient throughout the heat exchanger. However, this assumption is not valid when the heat transfer coefficient varies with the heat flux. Claesson [35] developed a correction factor relating the appropriate mean temperature difference with the ΔT_{ln}. He showed that the correction factor is negligible for moderate to high ΔT_{ln} ($>$ 4-5 K) and that the ΔT_{ln} approach is sufficiently accurate for predicting heat transfer in PHEs. At lower values, a correction factor can range between 0.5 and 0.95. It should be noted that the ΔT_{ln} in this study was $>$ 6 K and no correction factor was implemented.

The heat transfer rate is derived from a thermal energy balance on the water side:

$$Q = m_w C_{p,w} \Delta T_w \quad (6)$$

where m_w is the water mass flow rate measured by the Coriolis mass flow meter, $C_{p,w}$ is the water specific heat capacity taken at the average of the inlet and outlet temperatures and ΔT_w is the temperature difference measured at the inlet and outlet.

The average refrigerant heat transfer coefficient (h_r) of the BPHE is derived from the overall heat transfer coefficient as shown below. In this case fouling is assumed to be negligible.

$$h_r=\left(\frac{1}{U}-\frac{t}{k_{pt}}-\frac{1}{h_w}\right)^{-1} \quad (7)$$

Water-to-water experiments were first conducted before the water-to-refrigerant experiments. This allowed evaluation of the water-side heat transfer coefficient (h_w), see Eq. (8), and therefore subsequent evaluation of the heat transfer coefficient on the refrigerant side (h_r). The modified Wilson Plot technique [36] was used to evaluate h_w and the unknown constants C_1, C_2 and C_3 in Eq. (8). In each case the flow rate of the cold water was varied for a fixed flow rate on the hot water side.

$$h_w = C_1 Re_w^{C_2} Pr_w^{C_3} \frac{k_w}{D_h}\left(\frac{\mu_m}{\mu_{wall}}\right)^{0.14} \quad (8)$$

The exponent of the viscosity ratio was taken as 0.14 according to Kays et al. [37] However, this ratio is near unity for our experiments and was not included, see Eq. (9). The single-phase heat transfer correlations are expressed in terms of the Nusselt number for the hot side of the heat exchanger where water is commonly used as the heat transfer fluid.

$$Nu_w = C_1 Re_w^{C_2} Pr_w^{C_3} \tag{9}$$

The heat transfer coefficient is assumed to be the same on both sides, hot and cold, when the same fluid flows on both sides with an identical Reynolds number.

Pressure drop

The total pressure drop of the refrigerant is measured by a differential pressure transducer for the required range of flow rates and inlet pressures. The three-component model approach [32, 38] is used to evaluate the frictional pressure drop and subsequently the Fanning friction factor. In this case, the total or measured pressure drop (ΔP_{tt}) comprises of three components: the manifolds and ports pressure drop (ΔP_p), the elevation/gravity pressure drop (ΔP_g) and frictional pressure drop (ΔP_f) in the flow channels, that is:

$$\Delta P_{tt} = \Delta P_f + \Delta P_g + \Delta P_p \tag{10}$$

The pressure drop due to elevation is calculated by:

$$\Delta P_g = \rho g L_p \tag{11}$$

where ρ is taken at the mean inlet to outlet temperature, as with all properties.

A very widely cited equation by Shah and Focke [32] gives an estimation of the manifold pressure drop:

$$\Delta P_p = 1.5 \frac{n_p {G_p}^2}{2\rho_i} \tag{12}$$

where $G_p = \frac{m}{\left(\frac{\pi}{4}\right){D_p}^2}$ is the fluid mass velocity in the port, n_p is the number of passes on the given fluid side, and ρ_i is the density of the refrigerant at the inlet as proposed by Shah and Sekulic [39].

The acceleration pressure drop ΔP_a, given by Eq. (13) below, is negligible for single-phase liquids [38] and is excluded from the total pressure drop expression, especially given the small variation in the density between the inlet and outlet in the single-phase.

$$\Delta P_a = \left(\frac{1}{\rho_o} - \frac{1}{\rho_i}\right) G^2 \tag{13}$$

Accordingly, the frictional pressure drop can be computed by rearranging Eq. (10) that is:

$$\Delta P_f = \Delta P_{tt} - \Delta P_g - \Delta P_p \tag{14}$$

The following correlation is commonly applied to evaluate the Fanning friction factor (f) in the flow channels of PHEs, [40]:

$$\Delta P_{f=} \frac{4fLG^2}{2\rho D_h} \tag{15}$$

where $L = L_p$.

The definition of the characteristic length L in Eq. (15) is important here. The length L_p is used in this study in accordance with [17, 21, 29]. However it should be noted that other studies use the effective length L_{eff} [41]. L_p was chosen so as to include the triangular fluid distribution and collection areas that would otherwise be excluded in the analysis.

A relation between the friction factor and the Reynolds number is proposed, based on the experimental data. The Blasius equation cited in [42] is widely used for single-phase fully developed turbulent flow in smooth pipes. However, the friction factor in PHEs is known to be considerably higher compared to that in tubular exchangers [1], mainly due to the different flow geometry.

Calibration and uncertainty analysis

Instrument error and calibration

Table 3 gives the main features of the different measuring devices in the experimental rig. The uncertainty of the thermocouple was obtained using a calibration procedure with a precision thermometer (ASL F250 MK II) in a constant temperature bath using water.

Uncertainty analysis

The uncertainty of the experimental data was calculated using the method reported by Coleman and Steel [43]. The combined uncertainty of a measured parameter ϵ of the experimental data is composed of the systematic b_i and standard deviation s_x as shown in Eq. (16).

$$\epsilon^2 = {s_x}^2 + \sum_{i=1}^{K} {b_i}^2 \tag{16}$$

The propagated error on calculated parameters is evaluated using the Taylor Series Method where:

$$\epsilon_r = \left[\sum_i^k \left(\frac{\partial r}{\partial Y_i}\right)^2 {\epsilon_i}^2\right]^{1/2} \tag{17}$$

where $r = f(Y_i, \ldots . Y_k)$. These results are shown in Table 4.

Table 3. Specification of measuring devices in test facility.

Devices	Range	Accuracy
T- type thermocouples	−200 − 350 °C	± 0.1 K
Differential pressure transducer	0 − 0.344 bar	± 0.01 %
Inlet/outlet pressure transducers	0 − 10 bar	± 0.25 %
Refrigerant Coriolis flow meter	0 − 0.125 kg/s	± 0.035 %
Water Coriolis flow meter	0 − 0.30 kg/s	± 0.035 %

Table 4. Summary of uncertainty analysis.

Parameter	Uncertainty %
$\boldsymbol{Q_w}$	1.3 − 4.1
$\boldsymbol{U}$	1.6 − 5.3
$\boldsymbol{h_w}$	3.5 − 4.6
$\boldsymbol{h_r}$	4.6 − 6.9
$\boldsymbol{\Delta P_{tt}}$	1.8 − 3.3
$\boldsymbol{\Delta P_f}$	4.2 − 5.7
$\boldsymbol{f}$	5.4 − 7.3

The uncertainty associated with the use of the Modified Wilson Plot technique were accounted for in accordance with Sherbini et al. [44].

2.1. Steady state conditions

A steady-state condition was defined when the temperature, pressure and mass flow rate do not vary by more than ± 0.2 g/s for mass flow rate, ± 0.1 K for inlet/outlet temperatures on both sides and ± 0.01 bar for the inlet/outlet pressure on the refrigerant side over a period of 10 minutes. The length of time is recommended in [15] and helps to establish truly averaged data. Note that the heat exchanger was well insulated and at steady state the thermal balance on the water and refrigerant side was within ± 3%. The average value during this time is then computed for each parameter recorded. The time-averaged values were calculated to evaluate the single-phase heat transfer coefficient and frictional pressure drop on the refrigerant side.

Single-phase water to water experiments

As mentioned above, the Modified Wilson plot technique [45] was implemented to analyze the results for the water-water experiments and determine the heat transfer coefficient for the hot side. The analysis was performed according to the procedure described in Muley and Manglik [31] and Longo and Gasparella [16]. The method is used to determine the constant 'C_1' and the Reynolds number exponent 'C_2' in the heat transfer coefficient correlation of Eq. (8). The exponent of the Prandtl number was taken as 0.333 in agreement with [27, 32]. The viscosity ratio was taken as 1, see below for justification of the assumption. As mentioned before the overall heat transfer coefficient can be expressed as:

$$\frac{1}{U} = \frac{1}{h_{w,h}} + \frac{t}{k_{pt}} + \frac{1}{h_{w,c}} \tag{18}$$

where $h_{w,h}$ and $h_{w,c}$ are the heat transfer coefficients for the hot and cold water respectively and it is assumed that the same expression applies on both sides. To use linear regression, the expression for the heat transfer coefficient is rewritten by rearranging Eq. (8) for both the hot and cold side where:

$$h_{w,h} = C_1 \frac{k_{w,h}}{D_h} Re_{w,h}^{C_2} Pr_{w,h}^{0.33} \tag{19}$$

$$h_{w,c} = C_1 \frac{k_{w,c}}{D_h} Re_{w,c}^{C_2} Pr_{w,c}^{0.33} \tag{20}$$

Given the use of water on both sides of the heat exchanger, the constants C_1 is the same on both sides. Therefore, by substituting the terms of Eqs. (19) and (20) into Eq. (18), we get the expressions:

$$\left(\frac{1}{U} - \frac{t}{k_{pt}}\right) h_{w,h} = \frac{1}{C_1}\left(\frac{h_{w,h}}{h_{w,c}}\right) \tag{21}$$

Therefore

$$\left(\frac{1}{U} - \frac{t}{k_{pt}}\right) \frac{k_{w,h}}{D_h} Re_{w,h}^{C_2} Pr_{w,h}^{0.33} = \frac{1}{C_1} + \frac{\frac{k_{w,h}}{D_h} Re_{w,h}^{c_2} Pr_{w,h}^{0.33}}{\frac{k_{w,c}}{D_h} Re_{w,c}^{C_2} Pr_{w,c}^{0.33}} \tag{22}$$

Eq. (22) can be written in a linear from:

$$y = ax + b \tag{23}$$

where y and x are co-ordinates XX and YY as shown in Eq. (24).

$$\begin{aligned} YY &= \left(\frac{1}{U} - \frac{t}{k_{pt}}\right)\left[\frac{k_{w,h}}{D_h} Re_{w,h}^{c_2} Pr_{w,h}^{0.33}\right] \\ XX &= \left[\left(\frac{k_{w,h}}{k_{w,c}}\right)\left(\frac{Re_{w,h}}{Re_{w,c}}\right)^{C_2}\left(\frac{Pr_{w,h}}{Pr_{w,c}}\right)^{0.333}\right] \end{aligned} \tag{24}$$

A set of values for XX and YY from the experimental data can be fitted by linear regression for an initial guess of C_2 to determine coefficient C_1, calculated from the slope, where $a = \frac{1}{C_1}$ as shown in Figure 3. The best value for C_2 resulted from fitting the curve that best fits the experimental data, which is determined by the Coefficient of Multiple Determination (R-square). After successive iterations, the gradient and intercept were used to calculate; $C_2 = 0.89$ and $C_1 = 0.0488$. This correlation has a reliable regression result of $R^2 = 0.9958$.

Accordingly, the single-phase heat transfer coefficient on the water side is given by the following equation:

$$h_w = 0.0488\left(\frac{k_w}{D_h}\right) Re_w^{0.89} Pr_w^{0.333} \tag{25}$$

and in terms of the Nusselt number as:

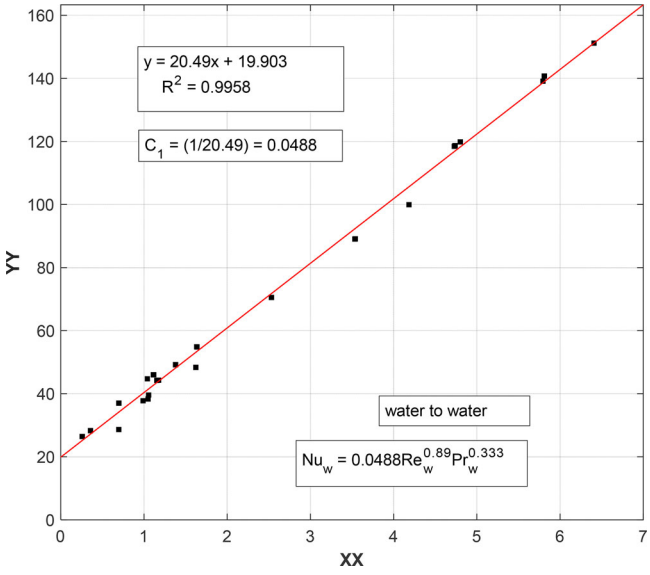

Figure 3. Modified Wilson Plot results for the calibration of the hot water side heat transfer coefficient.

$$Nu = 0.0488 Re_w^{0.89} Pr_w^{0.333} \tag{26}$$

The above correlation is applicable to a range of $80 < Re_w < 1600$ and $2.8 < Pr_w < 7.0$ for the plate geometry specified in Table 2. The viscosity correction factor, $\left(\frac{\mu_m}{\mu_{wall}}\right)^{0.14}$ in Eq. (8) is used to account for the large temperature differences between the surface/wall temperature and the mean temperature of fluid. This is more important in highly viscous fluids as the value usually deviates from 1. For example, Muley et al. [46] showed that for viscous fluids such as oil (Pr = 185), a ratio of $0.2 < \frac{\mu_m}{\mu_{wall}} < 0.8$ could result in a $3-20\%$ difference in the calculated Nusselt number and therefore the factor cannot be overlooked. The relationship in Eq. (27) was used to estimate the wall temperature (T_{wall}).

$$h_w(T_{wall} - T_{w,h}) = U(T_{w,c} - T_{w,h}) \tag{27}$$

The U-value was obtained from Eq. (4). The wall temperature was found to be only a $3-4$ K above the mean fluid temperature, therefore the correction ratio was ignored as $\left(\frac{\mu_m}{\mu_{wall}}\right)^{0.14} \approx 1$.

The developed water to water correlation is compared with others found in literature for BPHEs that are applicable to the experimental range and of a similar geometry used in this study. The validity of the comparison is based on the common definition of all the used parameters. The modification of these parameters is conducted through the following procedure in accordance with [16]. All correlations using the effective heat transfer area $\left(A_{eff} = A_p \times \phi\right)$ were modified by multiplying C_1 by ϕ, while those that used the hydraulic diameter $\left(\frac{2b}{\phi}\right)$ were modified by multiplying C_1 by ϕ^{1-C_2}. These conversions are shown in Appendix B in Eqs. (B1–B7). However, it should be noted that in some cases the definition of these parameters and the range for which the correlation is applicable are not reported [11, 12]. In such cases the range was taken as that of the current experimental work.

Table 5. The statistical assessment of the 11 examined BPHE correlations.

Correlation	Range	MAE
Hayes and Jokar [8]	–	59.4
Jokar et al. [9]	–	65.2
Lee et al. [10]	240< Re < 450; 5 < Pr < 10	17.9
Lee and Lee [11]	300< Re < 4000	73.1
Kim and Park [12]	950 < Re < 1400	7.4
Bogaert and Boles [13]	Re > 30	36.5
Han et al. [14]	–	56.0
Palmer et al. [15]	–	20.3
Longo and Gasparella [16]	200 < Re < 1200; 5 < Pr < 10	6.8
Longo et al. [17]	350 < Re < 1100; 5 < Pr < 10	21.9
Yang et al. [24]	50 < Re < 8000; 2 < Pr < 290	17.4

Table 5 summarizes the statistical assessment of the 11 examined correlations, while Figure 4 compares the experimental Nusselt number with that calculated using correlations in literature. Longo et al. [17] and Kim and Park [12] conducted their studies using 65° BPHEs and reported Nusselt number correlations for the single-phase experiments, using water as working fluid. Their results were in good agreement with the present experiments with the lowest Mean Absolute Error (MAE) of 6.8% and 7.4% respectively. The generalizedcorrelation proposed by Yang et al. [24] showed a reasonably good prediction accuracy with a MAE value of 17.4%. The correlation was developed from a wide data base and the Nusselt number was a function of the enlargement factor, aspect ratio and corrugation angle. Accordingly, the correlation can account for the effects of these geometric features appropriately.

Conversely, there are also considerably large deviations amongst the predicted values that could possibly be explained by the differences in geometrical parameters (aspect ratio, chevron angle and overall size), thermal boundary conditions and flow conditions and regimes. In many cases, these are not often mentioned causing for a lot of ambiguity in their applicability. For example, information regarding the range of the correlations in Palmer et al. [15] and Han et al. [14] was not reported. Similarly, Lee et al. [10] only disclosed information on the β and the ratio $\lambda/2b$ for which their numerical data was validated. Hence, this should be considered in this comparison.

$$Nu_w = 0.1449\ Re^{0.8414} Pr^{0.35} \tag{28}$$

It has previously been demonstrated that some GPHE correlations could be used to predict the

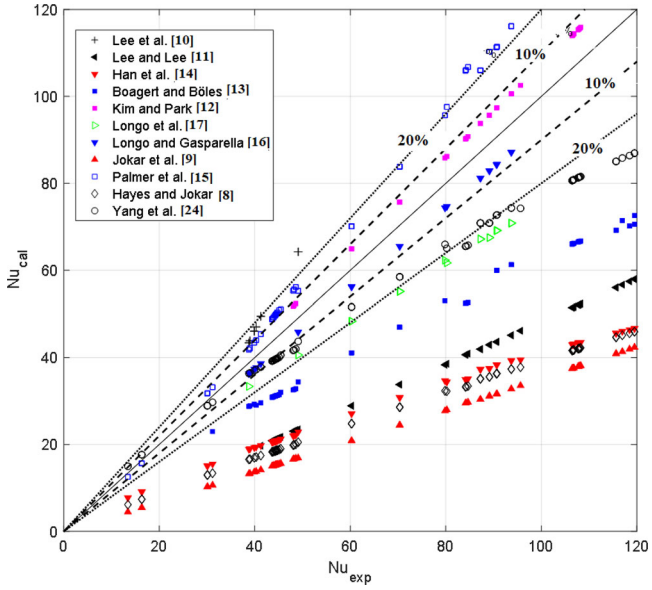

Figure 4. Comparison of experimental Nusselt number with calculated value from correlations in literature.

Table 6. Operating conditions for water-refrigerant tests.

Number of Tests	m_w [kg/s]	m_r [kg/s]	$P_{r,i}$ [bar]	$T_{r,i}$ [^{0}C]	T_{sat}[^{0}C]	$T_{w,i}$[^{0}C]	Q_w[kW]
134	0.05	0.038 – 0.078	1.9 – 2.1	14 – 27	36 – 39	21 – 50	0.5 – 2.0

performance of BPHEs [12]. Our experimental Nusselt number was also compared to that calculated by the Khan et al. [18] correlation developed for a symmetric 60° chevron GPHE using water as shown in below.

The Khan et al. [18] correlation under predicts slightly the experimental data with a good MAE of 3.4%, perhaps because of the slight differences in geometrical parameters. For example, $\gamma = 0.72$ and $\phi = 1.21$ in the plates used in the present case compared to $\gamma = 0.54$ and $\phi = 1.117$ in that used by Khan et al. More compact corrugations (corresponding to a higher aspect ratio) in the present case generate a greater flowing swirl, resulting in higher heat transfer rate as previously observed by Kim and Park [12]. This could explain why our data is underpredicted by the Khan et al. [18] correlation. It is worth mentioning that the Khan et al. [18] correlation predicted their experimental data within $\pm$ 1.8 – 2% in the Reynolds number range 500 – 2500 and the Prandtl number range 3.5 – 6.5.

On the other hand, a comparison by Kim and Park [12] using BPHEs with $\gamma = 0.72$ and 1.09, showed the Khan et al. [18] correlation over-predicted their data by 14.7 and 19.3% respectively. Given the slight variation in the results it is difficult to determine whether this is indeed coincidental, as thought by [12], given what we know of the discrepancies caused by the differences in the geometry.

Single phase water – refrigerant experiments

Heat transfer

The heat transfer analysis was conducted with the heat exchanger under steady state conditions. We assumed that the fluid flow rate and temperature remained uniform and undisturbed throughout the exchanger and that the overall heat transfer coefficient is constant. The outlet pressure and temperature of the refrigerant were monitored to ensure single-phase conditions were maintained. Experiments were carried out for a Reynolds number ranging from 700 to 1450 and Prandtl number from 4.5 to 4.9. Details of the experimental conditions are summarized in Table 6.

The refrigerant heat transfer coefficient was calculated using Eq. (7) while Eq. (25) was used to calculate the heat transfer coefficient on the water side. A linear increase in the refrigerant heat transfer coefficient with Reynolds number is shown in Figure 5. These values were found to be up to four to seven times larger than that of an equivalent flat plate channel (flow between two flat plates) predicted by Kakac and Shah [47] for $Re \leq 2000$ given as:

$$h = \left(\frac{k}{D_e}\right) 1.849 \left(\frac{L}{D_e}\right)^{-1/3} Re^{1/3} Pr^{1/3} \left(\frac{\mu}{\mu_w}\right)^{0.14} \quad (29)$$

The increase is due to the fact that the convective transport is enhanced substantially by the onset and growth of vortices in the furrows of the channels,

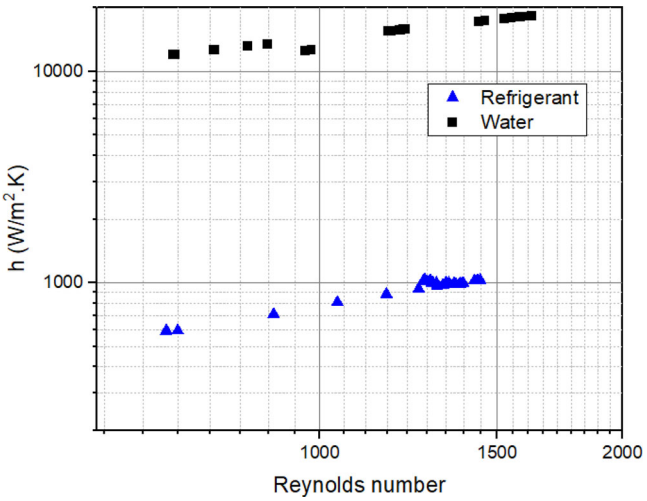

Figure 5. Refrigerant and water heat transfer coefficient with increasing Reynolds number.

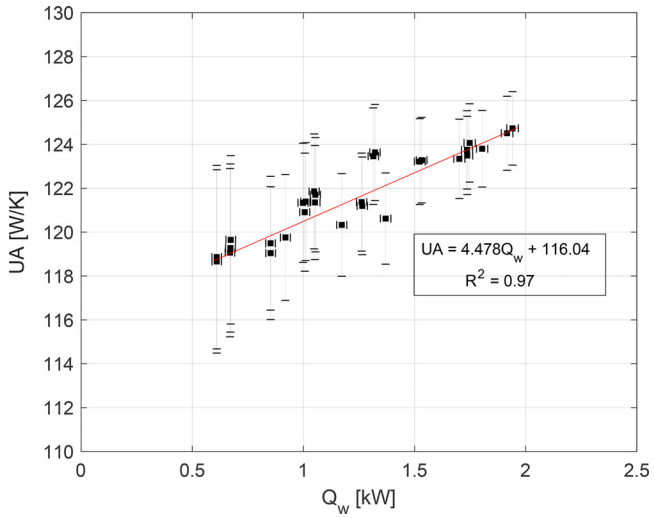

Figure 6. Increase in UA value with heat load for water side mass flux of 54 kg/m^2 s and refrigerant side mass flux of 95 kg/m^2 s.

which encompasses most of the bulk flow of the fluid [46]. At high corrugation angles such as that investigated here, the generated swirl flows promote a more uniform temperature distribution with steeper wall temperature gradients; thereby enhancing the convective heat transfer. The refrigerant side heat transfer coefficient was found to be up to 4.25 times lower than that of the water side making it the controlling resistance. The large difference is due to the effects of the thermal conductivity, which is one order of magnitude lower than that of water.

Similar observations were made by Hayes and Jokar [8] that found that the cold side using dynalene HC-50 resulted in a greater heat transfer coefficient in comparison to water due to the differences in fluid properties such as the Prandtl number ($10 < Pr < 250$ at temperatures between 50 °C and − 50 °C). It should be noted that the details of the fluid properties of dynalene HC-50 and the operating conditions for which the experiments were conducted were not reported, but were assumed and calculated from [48] for the purpose of this study.

Figure 6 indicates a slight increase in the UA value with the increasing heat load (Q_w) for a fixed flow rate of both fluids based solely on the variation of the water side inlet temperature. The UA value is a function of the two heat transfer coefficients and therefore the corresponding flow rates. However, the indicated small increase in the UA value could be attributed to the increased mean temperatures between the inlet and outlet leading to the decrease in density and viscosity of the refrigerant. As shown in Table 7, a 15 K

Table 7. Results for the increase in the in UA value.

	Q_w	UA	ΔT_{ln}	h_w	h_r	ρ_r	μ_r	T_r	Re_r	Pr
	1.05	121.8	8.6	1857	751	1277	3.2×10^{-4}	19.3	1270	4.75
	1.94	124.7	15.6	2200	761	1262	3.0×10^{-4}	25.3	1377	4.50
% change	84	2.3	80	18.5	1.5	1.2	6.3	31	8.4	5.3

increase in the water inlet temperature (a 0.89 kW increment in the heat load) resulted in a decrease in the viscosity and density by 6.3% and 1.2% respectively. This increased the Reynolds number by 8.4% and decreased the Prandtl number by 5.3% resulting in a small, 1.5%, increase in the refrigerant heat transfer coefficient and hence, the observed 2.3% increase in the UA value. Accordingly, the UA value is found to have a weak dependency on the inlet temperatures of the fluids but more so on the mass flux.

The water-to- water experiments resulted in a U value of $0.4 - 1.7\,\mathrm{kW/(m^2.\ K)}$ for a heat load of up to 3 kW and the flow rates studied. Similar values were observed by Huang et al. [23] for a low angle plate geometry ($\beta = 28°$) for a heat load of up to 45 kW. Yang et al. [24] who used a similar geometry and size ($A_p = 0.13 - 0.25\,\mathrm{m^2}$) of BPHEs observed slightly higher U values of $1 - 2.4\,\mathrm{kW/(m^2.\ K)}$, which could be attributed to the use of a 65 vol% ethylene glycol-water mixture on both sides of the heat exchanger. Despite the slightly lower thermal conductivity, the glycol-water mixture has higher Prandtl number ($50 \leq \mathrm{Pr} \leq 150$), therefore resulting in higher heat transfer coefficients. In contrast, the water-to-refrigerant tests were observed to produce lower U values ($0.45 - 0.6\,\mathrm{kW/(m^2.\ K)}$) as a result of the increased resistance on the cold side with the use of R1233zd(e).

With the same fluid on both sides of the heat exchanger, the fluid resistance or heat transfer coefficient is not dominated by any particular fluid. However, the use of a different fluid on the cold side implies that the U value is dependent on the lesser heat transfer coefficient and therefore on the fluid properties that determine its heat transfer coefficient, i.e. the thermal conductivity and Prandtl and Reynolds numbers. For example, a 30% increase in the Prandtl number would increase the heat transfer coefficient by 9%. Given that both the thermal conductivity and Prandtl number of R1233zd(e) do not vary drastically with pressure or temperature, the U value in the single phase can increase only as a function of the Reynolds number.

A linear regression analysis of the experimental data is used to determine the coefficients, C_1 and C_2 of the heat transfer coefficient and consequently the Nusselt correlation depicted in Eq. (30) in order to predict the single-phase heat transfer characteristics of R-1233zd(E) used in the present BPHE. The developed correlation predicted 97.2% of the experimental data within ± 10% error bands with a MAE value of 5.7%. A function of geometric parameters such as β or ϕ was not included in this correlation as only one BPHE was used here, and therefore the effect of different geometries cannot be accounted for.

$$Nu = 0.1381 Re^{0.75} Pr^{0.333}$$
$$700 \leq Re \leq 1450 \quad 4.5 \leq Pr \leq 4.9 \tag{30}$$

A fair comparison with existing correlations cannot be conducted as correlations were developed for different fluids, heat exchanger geometry and various flow conditions. Nevertheless, a comparison is made with a few existing correlations developed for BPHEs of equivalent geometry such as β, ϕ and within the operating range stated. In Figure 7 the current data is compared with the results (for the hot side) from Hayes and Jokar [8], Jokar et al. [9], Lee and Lee [11] and Han et al. [14]. However, it should be noted that both the Hayes and Jokar correlations for the hot and cold side (as indicated in the figure) were compared. Han et al. [14] investigated the boiling heat transfer and pressure drop of R410A and R22 in three BPHEs of $\beta = 45°$, 35° and 20°. The authors adopted the single-phase water-to-water correlation from Kim [49], which predicted our experimental data with a MAE of 4.45%, despite the fact that the correlation was developed for lower chevron angles. Single-phase experiments using water-to-water and water-to-dynalene in three different BPHEs (β= 60/60°, 27/60°, 27/27°) were conducted by Hayes and Jokar [8]. They proposed correlations for both the hot and cold side of the heat exchanger. Interestingly, their water-to- water hot side correlation showed a better prediction accuracy than that of the water-to-dynalene cold side with MAE values of 5.89% and 22.4%, respectively. Lee and Lee [11] examined the characteristics of pressure drop and heat transfer for chevron-type plate heat exchangers using unsteady numerical analysis with large-eddy simulation. Based on their numerical data they proposed a correlation to cover a geometry ranging from $15 \leq \beta \leq 75$, $2.0 \leq \frac{\lambda}{b} \leq 4$, and an operating range of $200 < \mathrm{Re} < 10000$ and $30 < \mathrm{Pr} < 50$ using water (Pr = 4.07), ethylene glycol (Pr = 13.52) and diesel fuel (Pr = 47.65). Their numerical results were validated

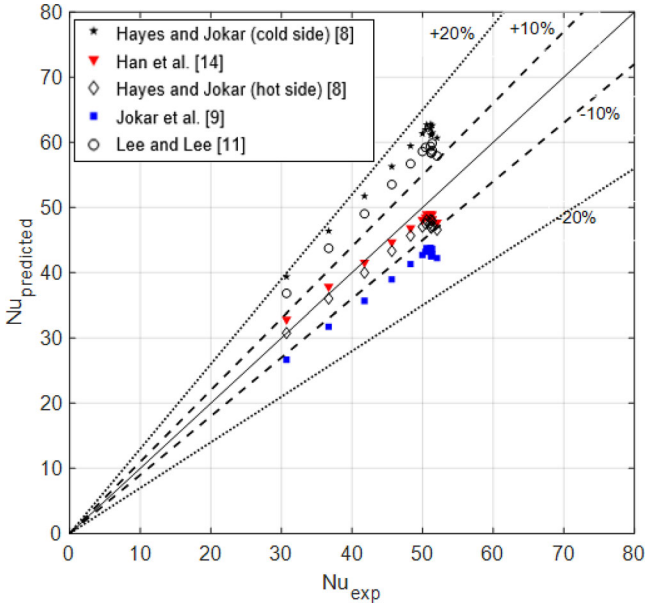

Figure 7. Comparison of prediction and experimental data using correlations in literature.

using their own experiments conducted using water and a plate geometry where $\beta = 60°$ and $\frac{\lambda}{b} = 2.8$ for a range of $300 < \mathrm{Re} < 4000$. Their results compared well with that of Muley and Manglik [31]. Their correlation also showed a good prediction accuracy of the present data $(\frac{\lambda}{b} = 3)$ with a MAE of 16.6%. On the other hand, the accuracy of the correlation by Lee and Lee [11] cannot be verified, since almost all the geometrical parameters were not reported. Similarly, for that of Hayes and Jokar [8], the Reynolds number and Prandtl number range of validity was not given. Unfortunately, there is a limited number of correlations in the open literature applicable to the range of data presented here. This reflects the lack of generalized and inclusive correlations.

Pressure drop

The pressure drop of the BPHE was recorded using a differential pressure transducer. The results reported are based on the characteristic length (L_p) for the evaluation of the friction factor as shown in Eq. (15). Figure 8 shows a linear dependency of the measured refrigerant pressure drop (ΔP_{tt}) with increasing Reynolds number. While BPHEs are known to enhance the heat transfer rates, the flow channels present a higher flow resistance and consequently higher pressure drop. For the present set of experimental data, the frictional pressure drop (ΔP_f) ranges from 25% to 65% of the total pressure drop measured. The pressure drop in the ports and manifolds (ΔP_p) was found to be less than 1% of the total. This result is consistent with some studies [19, 31], however Shah and Focke [32] mention that this could be as high as $10 - 30\%$ in some designs due to the variations in viscous forces of the fluid. Lee et al. [10] reported that the channel guide and number of channels had a significant effect on the port pressure. The channel guide, which distributes and collects the fluid at the inlet and outlet ports, induces swirling flow and vortices thus affecting the port pressure drop. The study also observed the port pressure drop to increase proportionally with the increase in the number of channels due to the increased resistance of flow through the channels guide.

The low pressure drop in the manifolds of the tested BPHE was attributed to the combination of a low number of channels on the refrigerant side, channel guide design, and fluid properties such as viscosity.

In Figure 9 the experimental results for the friction factor are compared with the few studies that report results related to the pressure drop in BPHEs and other well-known correlations for GPHEs. These correlations were selected for their similarities in geometry and application range. Similar to other studies, our data was also compared with the friction factor predicted from Kakac and Shah. [47] for the equivalent flat plate, which showed significant disagreement and therefore not included in the figure. This is because the corrugated flow channels significantly increase the friction losses in PHEs in comparison to flat plates. The Bond [22] and Huang et al. [23] correlations, obtained for GPHEs, agree with the results of

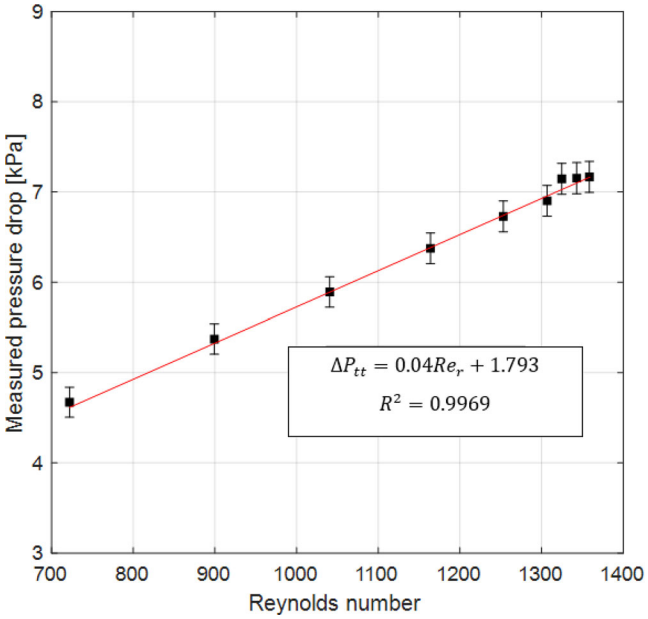

Figure 8. Refrigerant total pressure drop versus Reynolds number.

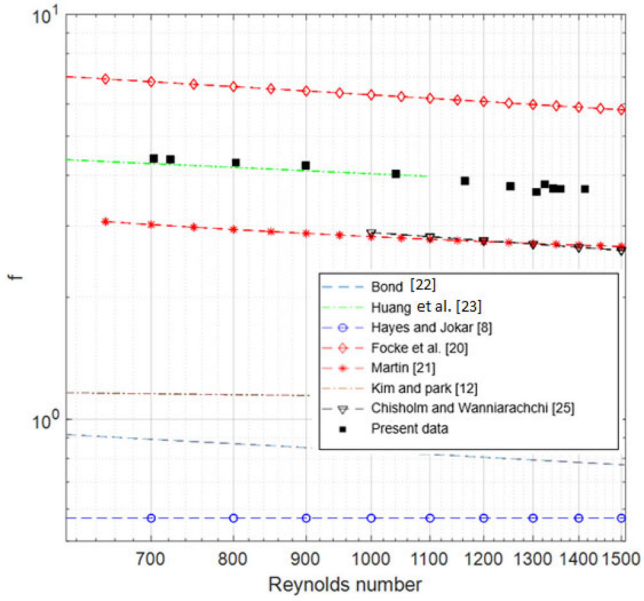

Figure 9. Comparison of refrigerant friction factor with previous studies.

the present experiments fairly well, however a general comparison shows large differences between various correlations. For example, the highest predicted value by Focke et al. [20] was up to 17 times higher than the lowest value predicted by Hayes and Jokar [8]. The Focke et al. [20] correlation has the highest predicted results because of the large differences in geometry, for example $D_h = 10\,\text{mm}$ in the scaled-up surfaces employed by the authors compered to $D_h = 2\,\text{b} = 4.34\,\text{mm}$ in the present case. Martin [21] conducted a theoretical analysis on the flow distribution and pressure drop in PHEs, based on the assumption that the pressure losses in the manifolds is negligible which is a questionable assumption.

The disagreement in the proposed correlations can be explained by several factors: (i) the plate geometries differ with that used in the present study, whether it is the chevron angle, the plate spacing, hydraulic diameter or plate size (ii) the type of working fluid and (iii) inconsistently defined/used parameters such as the hydraulic/equivalent diameter and characteristic length used to calculate the friction factor (Eq. (15)). Despite the wide use of Eq. (15), when applied to PHEs of different geometries, the friction factor calculated by the model has been found to vary by put to $50-100\%$. For example, Solotych [50] reported two different correlations for R245fa and R236a in turbulent flow using the same PHEs. This implies that the model does not correctly account for the strong influence of physical properties of the working fluid. Consequently, the f - correlation found for a specific unit, may perhaps be valid for its specific design and experimental conditions.

It is also worth noting that the transition to turbulent flow is reported to be different by various researchers. For example, while Muley and Manglik [31] and Hessami [45] reported transitional range to occur at $500 < \text{Re} < 800$ and $600 < \text{Re} < 1300$ respectively, others like Focke et al. [20] and Thonon [51] considered it to occur at $\text{Re} < 1000$. It should be noted that with the exception of Thonon, these authors based their calculations for the Reynolds

number on the equivalent diameter. Perhaps the use of the hydraulic number in addition to the other geometrical parameters could explain the lack of consensus. The present data does not imply a transition region and therefore we assumed the flow was entirely in the turbulent region.

From Appendix A it is evident that the pressure drop in BPHEs has been studied even less than that in GPHEs. Kim and Park [12] compared their data with that of GPHEs reported by authors like Muley and Manglik [31], Chisholm and Wanniarachchi [25] and Heavner et al. [52] and found that the correlations under-predicted the friction factor. The brazing points in BPHEs contribute to further restriction and/or disruption to the flow and increase the friction losses along the channel. Therefore, these correlations developed for GPHEs cannot be regarded as general solutions for the pressure drop inside BPHEs.

Conclusions

The single-phase heat transfer and pressure drop characteristics of R1233zd(e) using a commercial BPHE were investigated. Initial water-to-water experiments were conducted to evaluate the single-phase heat transfer coefficient on the hot side using the Modified Wilson plot. The experiments covered a range of Reynolds number from 80 to 1600 and Prandtl number from 2.8 to 7.0, where fluid properties were taken at the mean temperature (average of inlet and outlet). Subsequent experiments were conducted with a water-to-R1233zd(e) covering a refrigerant range of Reynolds number from 700 to 1450 and Prandtl number from 4.5 to 4.9, again with the properties calculated at the average on the inlet and outlet temperatures of the water and the refrigerant.

The experimental data for both data sets were used to compare and assess the prediction accuracy of the most relevant correlations in literature. Some correlations provided a good prediction accuracy, within a ± 20% error margin, while others showed considerable large differences. The lack of agreement was explained by the complexity of the flow channels, in terms of the corrugation geometry and the fact that the heat transfer coefficient could be function of the large number of combinations of parameters such as the aspect ratio, chevron angle and surface enlargement factor. Accordingly, new correlations are proposed, i.e. (Eq. (25)) for the single-phase heat transfer coefficient for the hot (water) side and the cold (refrigerant) side (Eq. (30)) for the geometry and range investigated. The refrigerant heat transfer correlation predicted 97% of all data within the ± 10% error bands at a MAE value of 5.7%.

It must be mentioned that a general correlation applicable to all chevron angles, and operating conditions in the single phase is not yet available. Although there is a widely felt need for such a correlation, BPHEs continue to be proprietary in nature making it a very difficult task to summarize a single correlation valid for different geometries and working fluids. Therefore, most correlations are still only fitted for a specific experimental geometry and operating conditions. As previously mentioned, the chevron plate pattern may be the most widely used, but there is no industry standard with several corrugation patterns from different manufacturers. Correlations can be chosen based on plate geometry and range of validity but used as rough estimates only. Where higher accuracy is required, vigorous testing of individual heat exchangers is preferable. Further work is recommended to reach a more generally accepted correlation both for heat transfer rates and friction factor prediction. For now, the correlations proposed here can be recommended based both on carefully validated experiments and agreement with past correlations.

Disclosure statement

No potential conflict of interest was reported by the author.

Funding

This research was supported by EPSRC Grant EP/P004709/1. The help of Costas Xanthos in constructing and maintaining the test rig is appreciated.

Notes on contributors

Angela Mutumba graduated with an MEng Degree in 2012 from the Mechanical Engineering Department at Queen Mary University, London, UK. With a full scholarship she joined Prof. Dongsheng Wen's research group at the University of Leeds in 2014 where she attained a PhD in direct contact liquid heat transfer in a cryogenic engine in 2019. She later joined Prof. Karayiannis's research group as a Research Fellow working on single and two-phase flow boiling in heat exchangers. She is currently a research Engineer at Michell Instruments, UK.

Francesco Coletti holds a Laurea degree in Chemical Engineering from the University of Padova, Italy, an MSc and PhD in Chemical Engineering from Imperial College London. Upon graduation, he worked as R&D specialist in Praxair Inc (now Linde) in Buffalo, NY. He is currently a co-founder and the CEO of Hexxcell Ltd. and a Senior Lecturer (part-time) in Chemical Engineering at Brunel University London. His expertise and research interests are at the intersection of the two exciting fields of Process Systems Engineering and Heat Transfer with focus on modeling, optimization, and predictive maintenance of energy systems. In these fields, he has published over 50 peer-reviewed papers and conference proceedings, 2 Special Issues, 2 patents and a monograph. He is also the Executive Editor of Heat Exchanger Design Handbook, a Director of the Fuels & Petrochemical Division of the American Institution of Chemical Engineers (AIChE), the Secretary of the UK National Heat Transfer Committee and a Member of the Assembly for International Heat Transfer Conferences. He initiated, and is the Chair of, the Topical Series on Heat Exchangers held every two years at the AIChE Spring Meeting.

Alex Reip is an award-winning tech entrepreneur working in several sectors including nanotechnology, cleantech, biotech and B2B voice recognition. He works with several startups around the UK to help their early-stage growth, through investment readiness and development of their ongoing technology strategy. He is a co-founder and now CTO of Oxford nanoSystems (OnS), a nanotechnology company developing energy efficient coatings for sectors including HVACR and Electrolyzers. He is also a Non-Executive Director of the Net Zero Technology Center. He has a PhD in nanotechnology from Brunel University and has over 15 years' experience in the development and commercialization of advanced nanomaterials. He is a Charted Chemist and Fellow of the Royal Society of Chemistry and a member of its Professional Standards Board. He is also a member of the NCFE technical advisory board working on the Science T-Level assessments. As a Royal Society Entrepreneur in Residence for Brunel University, he also works to develop an Open Innovation approach to commercialization, advises the spinouts and is a member of the university's Commercialization Panel.

Mohamed M. Mahmoud graduated in 1998 from the Mechanical Engineering Department, Faculty of Engineering, Zagazig University, Egypt. He was employed as an assistant lecturer in the Environmental Engineering Department in the same university since 1999. He received his M.Sc. in 2004 in the field of biomass combustion from Zagazig University. He joined Prof. Karayiannis's research group, as a PhD student, at Brunel University, London, UK, in 2007 and got his PhD in 2011 in two-phase flow boiling heat transfer in small- to micro diameter tubes. He worked as a lecturer in the Environmental Engineering Department from 2011 to 2018. Currently, he is an associate professor in the Environmental Engineering Department, Zagazig University. His research interests include pool boiling and flow boiling heat transfer in microsystems, solid waste/biomass thermal treatment for biofuel production, and thermal desalination systems.

Tassos Karayiannis studied at the City University London and the University of Western Ontario. He started his career as a researcher at Southampton University and later as a British Technology Group Researcher at City University. Subsequently he worked at London South Bank University and joined Brunel University London in 2005, where he is now Professor of Thermal Engineering, Leader of the Two-Phase Flow and Heat Transfer Group and Director of the Energy Efficient and Sustainable Technologies Research Center. He has carried out fundamental and applied research in a number of single-and two-phase heat transfer areas. He has published more than 260 chapters in books, papers and industrial reports. He chairs the Committee of the International Conference Series on Micro and Nanoscale Flows now in its 7th edition and co-chairs the 7th World Congress on Momentum, Heat and Mass Transfer. He is a Fellow of the EI and the IMechE, Member of the Assembly for International Heat Transfer Conferences and the Chairman of the UK National Heat Transfer Committee.

ORCID

Francesco Coletti http://orcid.org/0000-0001-9445-0077
Tassos G. Karayiannis http://orcid.org/0000-0002-5225-960X

References

[1] K. Thulukkanam, *Heat Exchanger Design Handbook*. 2nd ed. Boca Raton, Florida, USA: CRC Press, 2013.
[2] F. Molés, et al., "Low GWP alternatives to HFC-245fa in organic rankine cycles for low temperature heat recovery: HCFO-1233zd-E and HFO-1336mzz-Z," *Appl. Therm. Eng.*, vol. 71, no. 1, pp. 204–212, 2014. DOI: 10.1016/j.applthermaleng.2014.06.055.
[3] J. Yang, Z. Ye, B. Yu, H. Ouyang and J. Chen, "Simultaneous experimental comparison of low-GWP refrigerants as drop-in replacements to R245fa for Organic Rankine cycle application: R1234ze(Z), R1233zd(E), and R1336mzz(E)," *Energy*, vol. 173, pp. 721–731, 2019. DOI: 10.1016/j.energy.2019.02.054.
[4] L. Wang, B. Sundén and R. M. Manglik, *Plate Heat Exchangers: Design, Applications and Performance*, Southampton, UK: WIT Press, 2007.
[5] W. Li and P. Hrnjak, "Compensating for the end-plate effect on heat transfer in brazed plate heat

exchangers," *Int. J. Refrig.*, vol. 126, pp. 99–108, 2021. DOI: 10.1016/j.ijrefrig.2021.01.019.

[6] C. Jiang, et al., "Heat transfer enhancement of plate heat exchangers with symmetrically distributed capsules to generate counter-rotating vortices," *Int. J. Heat Mass Transf.*, vol. 151, pp. 119455, 2020. DOI: 10.1016/j.ijheatmasstransfer.2020.119455.

[7] X. Zhu and F. Haglind, "Relationship between inclination angle and friction factor of chevron-type plate heat exchangers," *Int. J. Heat Mass Transf.*, vol. 162, pp. 120370, 2020. DOI: 10.1016/j.ijheatmasstransfer.2020.120370.

[8] N. Hayes and A. Jokar, "Dynalene/water correlations to be used for condensation of CO2 in brazed plate heat exchangers," *ASHRAE Trans. Ann. Meeting, Louisville, Kentucky, USA*, vol. 115, no. part 2, pp. 599–616, 2009.

[9] A. Jokar, M. H. Hosni and S. J. Eckels, "Dimensional analysis on the evaporation and condensation of refrigerant R-134a in mini-channel plate heat exchangers," *Appl. Therm. Eng.*, vol. 26, no. 17–18, pp. 2287–2300, 2006. DOI: 10.1016/j.applthermaleng.2006.03.015.

[10] D. C. Lee, D. Kim, W. Cho and Y. Kim, "Evaporation heat transfer and pressure drop characteristics of R1234ze(E)/R32 as a function of composition ratio in a brazed plate heat exchanger," *Int. J. Heat Mass Transf.*, vol. 140, pp. 216–226, 2019. DOI: 10.1016/j.ijheatmasstransfer.2019.06.004.

[11] J. Lee and K.-S. Lee, "Friction and Colburn factor correlations and shape optimization of chevron-type plate heat exchangers," *Appl. Therm. Eng.*, vol. 89, pp. 62–69, 2015. DOI: 10.1016/j.applthermaleng.2015.05.080.

[12] M. B. Kim and C. Y. Park, "An experimental study on single phase convection heat transfer and pressure drop in two brazed plate heat exchangers with different chevron shapes and hydraulic diameters," *J. Mech. Sci. Technol.*, vol. 31, no. 5, pp. 2559–2571, 2017. DOI: 10.1007/s12206-017-0454-0.

[13] R. Bogaert and A. Böles, "Global performance of a prototype brazed plate heat exchanger in a large Reynolds number range," *Exp. Heat Transf.*, vol. 8, no. 4, pp. 293–311, 1995. DOI: 10.1080/08916159508946508.

[14] D.-H. Han, K.-J. Lee and Y.-H. Kim, "Experiments on the characteristics of evaporation of R410A in brazed plate heat exchangers with different geometric configurations," *Appl. Therm. Eng.*, vol. 23, no. 10, pp. 1209–1225, July 2003. DOI: 10.1016/S1359-4311(03)00061-9.

[15] S. C. Palmer, W. V. Payne and P. A. Domanski, "Evaporation and condensation heat transfer performance of flammable refrigerants in a brazed plate heat exchanger", NIST Interagency/Internal Rep. (NISTIR), National Institute of Standards and Technology, Gaithersburg, Maryland, USA, Rep. 6541, 2000.

[16] G. A. Longo and A. Gasparella, "Heat transfer and pressure drop during HFC refrigerant vaporisation inside a brazed plate heat exchanger," *Int. J. Heat Mass Transf.*, vol. 50, no. 25–26, pp. 5194–5203, 2007. DOI: 10.1016/j.ijheatmasstransfer.2007.07.001.

[17] G. A. Longo, A. Gasparella and R. Sartori, "Experimental heat transfer coefficients during refrigerant vaporisation and condensation inside herringbone-type plate heat exchangers with enhanced surfaces," *Int. J. Heat Mass Transf.*, vol. 47, no. 19–20, pp. 4125–4136, 2004. DOI: 10.1016/j.ijheatmasstransfer.2004.05.001.

[18] T. S. Khan, M. S. Khan, M.-C. Chyu and Z. H. Ayub, "Experimental investigation of single phase convective heat transfer coefficient in a corrugated plate heat exchanger for multiple plate configurations," *Appl. Therm. Eng.*, vol. 30, no. 8–9, pp. 1058–1065, 2010. DOI: 10.1016/j.applthermaleng.2010.01.021.

[19] T. S. Khan, M. S. Khan and Z. H. Ayub, "Single-phase flow pressure drop analysis in a plate heat exchanger," *Heat Transf. Eng.*, vol. 38, no. 2, pp. 256–264, 2017. DOI: 10.1080/01457632.2016.1177430.

[20] W. W. Focke, J. Zachariades and I. Olivier, "The effect of the corrugation inclination angle on the thermohydraulic performance of plate heat exchangers," *Int. J. Heat Mass Transf.*, vol. 28, no. 8, pp. 1469–1479, 1985. DOI: 10.1016/0017-9310(85)90249-2.

[21] H. Martin, "A theoretical approach to predict the performance of chevron-type plate heat exchangers," *Chem. Eng. Process. Process Intensif.*, vol. 35, no. 4, pp. 301–310, 1996. DOI: 10.1016/0255-2701(95)04129-X.

[22] B. M. P, "Plate heat exchangers for effective heat transfer," *Chem. Eng.*, vol. 367, pp. 162–166, 1981.

[23] J. Huang, T. J. Sheer and M. Bailey-McEwan, "Performance of plate heat exchangers used as refrigerant liquid-overfeed evaporators," Proced. of the 14th Int. Heat Transfer Conf. IHTC14, August 8–13, Washington, DC, USA, IHTC14-22095, 2010. DOI: 10.1115/IHTC14-22095.

[24] J. Yang, A. Jacobi and W. Liu, "Heat transfer correlations for single-phase flow in plate heat exchangers based on experimental data," *Appl. Therm. Eng.*, vol. 113, no. 25, pp. 1547–1557, 2017. DOI: 10.1016/j.applthermaleng.2016.10.147.

[25] D. Chisholm and A. S. Wanniarachchi, "Maldistribution in single-pass mixed channel plate heat exchangers," in *Compact Heat Exchangers for Power and Process Industry*, vol. 201, New York: HTD-ASME, 1992, pp. 95–99.

[26] Z. H. Ayub, "Plate heat exchanger literature survey and new heat transfer and pressure drop correlations for refrigerant evaporators," *Heat Transf. Eng.*, vol. 24, no. 5, pp. 3–16, 2003. DOI: 10.1080/01457630304056.

[27] F. W. Dittus and L. M. K. Boelter, "Heat transfer in automobile radiators of the tubular type," *Int. Commun. Heat Transf.*, vol. 12, no. 1, pp. 3–22, 1985. DOI: 10.1016/0735-1933(85)90003-X.

[28] K. Okada, et al., "Design and heat transfer characteristics of a new plate heat exchanger," *Heat Transf. Japan. Res.*, vol. 1, no. 1, pp. 90–95, 1972.

[29] Y. Y. Hsieh and T. F. Lin, "Saturated flow boiling heat transfer and pressure drop of refrigerant R-410A in a vertical plate heat exchanger," *Int. J. Heat Mass Transf.*, vol. 45, no. 5, pp. 1033–1044, 2002. DOI: 10.1016/S0017-9310(01)00219-8.

[30] M. Faizal and M. R. Ahmed, "Experimental studies on a corrugated plate heat exchanger for small temperature difference applications," *Exp. Therm. Fluid Sci.*, vol. 36, pp. 242–248, 2012. DOI: 10.1016/j.expthermflusci.2011.09.019.

[31] A. Muley and R. M. Manglik, "Experimental study of turbulent flow heat transfer and pressure drop in a plate heat exchanger with chevron plates," *J. Heat Transf.*, vol. 121, no. 1, pp. 110– 117, 1999. DOI: 10.1115/1.2825923.

[32] R. K. Shah and W. Focke, "Plate heat exchangers and their design theory," in *Heat Transfer Equipment Design*. Washington, DC: Hemisphere, 1988.

[33] T. S. Khan, M. S. Khan, M.-C. Chyu, Z. H. Ayub and J. A. Chattha, "Review of heat transfer and pressure drop correlations for evaporation of fluid flow in plate heat exchangers (RP-1352)," *HVAC&R Res*, vol. 15, no. 2, pp. 169–188, 2009. DOI: 10.1080/10789669.2009.10390832.

[34] G. A. Longo, "Vaporization of the low GWP refrigerant HFO1234yf inside a brazed plate heat exchanger," *Int. J. Refrig.*, vol. 35, no. 4, pp. 952–961, 2012. DOI: 10.1016/j.ijrefrig.2011.12.012.

[35] J. Claesson, "Correction of logarithmic mean temperature difference in a compact brazed plate evaporator assuming heat flux governed flow boiling heat transfer coefficient," *Int. J. Refrig.*, vol. 28, no. 4, pp. 573–578, 2005. DOI: 10.1016/j.ijrefrig.2004.09.011.

[36] J. Fernández-Seara, F. J. Uhía, J. Sieres and A. Campo, "A general review of the Wilson plot method and its modifications to determine convection coefficients in heat exchange devices," *Appl. Therm. Eng.*, vol. 27, no. 17–18, pp. 2745–2757, 2007. DOI: 10.1016/j.applthermaleng.2007.04.004.

[37] W. M. Kays, B. Weigand and M. E. Crawford, *Convective Heat and Mass Transfer*, 4th ed. Boston: McGraw-Hill Higher Education, 2005,

[38] S. Gusew and R. Stuke, "Pressure drop in plate heat exchangers for single-phase convection in turbulent flow regime: experiment and theory," *Int. J. Chem. Eng.*, vol. 2019, pp. 1–11, 2019. DOI: 10.1155/2019/3693657.

[39] R. K. Shah, R. K and D. P. Sekulic, *Fundamentals of Heat Exchanger Design*. New Jersey: John Wiley & Sons, 2012.

[40] R. L. Amalfi, F. Vakili-Farahani and J. R. Thome, "Flow boiling and frictional pressure gradients in plate heat exchangers. Part 1: Review and experimental database," *Int. J. Refrig.*, vol. 61, pp. 166–184, 2016. DOI: 10.1016/j.ijrefrig.2015.07.010.

[41] I. Gherasim, M. Taws, N. Galanis and C. T. Nguyen, "Heat transfer and fluid flow in a plate heat exchanger part I. Experimental investigation," *Int. J. Therm. Sci.*, vol. 50, no. 8, pp. 1492–1498, 2011. DOI: 10.1016/j.ijthermalsci.2011.03.018.

[42] B. R. Munson, D. F. Young, T. H. Okiishi and W. W. Huebsch, *Fundamentals of Fluid Mechanics*, 6th ed. John Wiley & Sons, Inc., New Jersey, USA, 2009.

[43] H. W. Coleman and G. Steele, *Experimentation, Validation, and Uncertainty Analysis for Engineers*, 3rd ed. John Wiley & Sons, Inc., New Jersey, USA, 2009.

[44] A. I. Sherbini, A. Joardar and A. Jacobi, "Modified Wilson-Plot technique for heat exchanger performance: Strategies for minimizing uncertainty in data reduction," Proceed. of the 2004 Int. Refrig. Air Cond. Conf. at Purdue, July 12 – 15, 2004, Purdue University, West Lafayette, Indiana, USA, vol. 1, paper, pp. 627. Available: http://docs.lib.purdue.edu/cgi/viewcontent.cgi?article=1626&context=iracc.

[45] M. A. Hessami, "An experimental investigation of the performance of cross-corrugated plate heat exchangers," *J. Enh. Heat Transf.*, vol. 10, no. 4, pp. 379– 394, 2003. DOI: 10.1615/JEnhHeatTransf.v10.i4.30.

[46] A. Muley, R. M. Manglik and H. M. Metwally, "Enhanced heat transfer characteristics of viscous liquid flows in a chevron plate heat exchanger," *J. Heat Transf.*, vol. 121, no. 4, pp. 1011–1017, 1999. DOI: 10.1115/1.2826051.

[47] S. Kakaç and R. K. Shah, *Handbook of Single Phase Convective Heat Transfer*. New Jersey, USA: John Wiley & Sons, Inc., 1987.

[48] Dynalene, Online website available at: https://www.dynalene.com/fluid-property-calculation/ Accessed June 2021.

[49] Y. S. Kim, "An experimental study on evaporation heat transfer characteristics and pressure drop in plate heat exchanger," MSc thesis, Yonsei University, South Korea, 1999.

[50] V. Solotych, "Two-phase heat transfer mechanisms within plate heat exchangers: Experiments and modeling," PhD thesis, University of Maryland, College Park, USA, 2016.

[51] B. Thonon, "Design method for plate evaporators and condensers," 1st Int. Conf. Process Intensif. Chem. Ind., Organized and Sponsored by BHR Group Ltd., Antwerp, Belgium, Dec. 6–8, 1995.

[52] R. L. Heavner, H. Kumar and A. S. Wanniarachchi, "Performance of industrial plate heat exchanger – Effect of chevron angle," in *Heat Transfer – Atlanta 1993 (AIChE Symp. Ser., no. 295, vol. 89, pp. 262–267)*. New York, USA: American Institute of Chemical Engineering, 1993.

Appendix A

Table A1. List of the recent relevant studies on GPHEs and BPHEs found in open literature and developed correlations. G: GPHE and B: BPHE.

Author	L_p	W	ϕ	β°	b	λ	D_h	Np	$N_{ch,r}$	$N_{ch,w}$	(A)	Fluid	Correlation
Hayes and Jokar [8] (B)	476.25	127	1.2	60/60	2	6.27 6.19 6.03	$2b$		3	3	$A_p \times \phi$	Water-Water Dynalene-Water	$Nu_h = 0.134Re^{0.712}Pr^{0.333}\left(\frac{\mu}{\mu_{wall}}\right)^{0.14}$ $Nu_c = 0.177Re^{0.744}Pr^{0.333}\left(\frac{\mu}{\mu_{wall}}\right)^{0.14}$ $f = 0.57$
				27/60									$Nu_h = 0.214Re^{0.698}Pr^{0.333}\left(\frac{\mu}{\mu_{wall}}\right)^{0.14}$ $Nu_c = 0.278Re^{0.745}Pr^{0.333}\left(\frac{\mu}{\mu_{wall}}\right)^{0.14}$ $f = 21.40Re^{-0.46}$
				27/27									$Nu_h = 0.240Re^{0.724}Pr^{0.333}\left(\frac{\mu}{\mu_{wall}}\right)^{0.14}$ $Nu_c = 0.561Re^{0.726}Pr^{0.333}\left(\frac{\mu}{\mu_{wall}}\right)^{0.14}$ $f = 3.15Re^{-0.08}$
Jokar et al.[9] (B)	311	112		60	2		$2b$	34 40 54				Water − 50 % gycol-water	$Nu = 0.089Re^{0.79}Pr^{0.33}$ $f = 6.431Re^{-0.25}$
Lee et al. (B) [10]	234	117		60	1.95	7.5	$\frac{2b}{\phi}$					Water R1234ze(E) Water -R32 Water – water	$Nu_w = 0.02628Re^{1.21}Pr^{0.333}$ $240 < Re < 450 \;\; 5 < Pr < 10$
Lee and Lee [11] (B)				60									$Nu_w = 0.1312Re^{0.78}Pr^{0.333}$ $f = 3.7235Re^{-0.2113}$ $300 < Re < 4000$
Kim and Park [12] (B)	243 269	113 83	1.221 1.166	65	2 1.3 1.02	7.3 7.2	$\frac{2b}{\phi}$	20			$A_p \times \phi$	Water	$Nu_w = 0.1452\phi^{2.079}Re^{0.7640}Pr^{0.333}$, $500 < Re < 800$ $f = \phi^4\left(0.6796\phi Re^{-0.0551} + 0.2\right)$ for type I BPHE at $950 < \mathrm{Re} < 1400$, for type II at $450 < \mathrm{Re} < 1300$
Bogaert and Boles [13] (B)	236	113	1.2	22	2		$2b$	12	7	6		Oil - Industrial water	$Nu = 0.34641Re^{0.6636}Pr^{c}\left(\frac{\mu}{\mu_{wall}}\right)^{\frac{0.3}{(Re+6)^{0.125}}}$ $c = \; 0.333e^{\frac{6.4}{(Pr+30)}}$ for $Re > 230$ c = 0.35 for oil c = 0.4 for industrial water $f = 67.67 \times 10^7 Re^{-0.308}$ $30 < Re < 200$
Han et al. [14] (B)	476	115	1.17	20 35 45	2.55	4.9 − 7.0	$\frac{2b}{\phi}$	4	2	3		Water – water	$Nu_w = \left(\frac{\pi}{2} - \beta\right)^{0.09}0.295Re^{0.64}Pr^{0.32}$
Palmer et al. [15] (B)	524	116		–	2		$2b$	28	14	15		Water – water	$Nu_w = 0.16Re^{0.89}Pr^{0.3}$
Longo and Gasparella [16] (B)	278	72	1.24	65	2		$2b$		5	4	A_p	Water - R22, R290, R290/600A, R32/152A Water – water Water - R134a R236a	$Nu_w = 0.277 \; Re^{0.766}Pr^{0.33}$ $200 < Re < 1200 \;\; 5 < Pr < 10$

(*Continued*)

Table A1. Continued.

Author	L_p	W	ϕ	β°	b	λ	D_h	Np	$N_{ch,r}$	$N_{ch,w}$	(A)	Fluid	Correlation
												R410a R600a R290 R1270 R1234fy R152a R404a	
Longo et al. [17] (B)	290	75	1.24	65	2	8	2b	4	1	2		Water – water	$Nu_w = 0.46\ Re^{0.66}Pr^{0.33}$
												R22	$350 < Re < 1100\ 5 < Pr < 10$
Khan et al. [18, 19] (G)	565	185	1.117	30/30 30/60 60/60	3.7 3.4 2.8	13.25 6.25	$\frac{2b}{\phi}$				$A_p \times \phi$	Water	$Nu_w = 0.1368\ Re^{0.7424}Pr^{0.35}\left(\frac{\mu}{\mu_w}\right)^{0.14}$ $f = 1.76Re^{-0.26}$ $Nu_w = 0.1437Re^{0.7810}Pr^{0.35}\left(\frac{\mu}{\mu_w}\right)^{0.14}$ $f = 2.07Re^{-0.27}$ $Nu_w = 0.1449\ Re^{0.8414}Pr^{0.35}\left(\frac{\mu}{\mu_w}\right)^{0.14}$ $f = 34.43Re^{-0.5}$
Focke et al. [20] (G)			1.464	$0-60$	2.5	10	2 b				A_p		$500 < Re < 2500\ 3.5 < Pr < 6.5$ For $\beta = 60^\circ$ $Nu = \begin{cases} 1.89Re^{0.46}Pr^{0.5}, & 20 < Re < 150 \\ 0.57Re^{0.7}Pr^{0.5}, & 150 < Re < 600 \\ 1.12Re^{0.6}Pr^{0.5}, & 600 < Re < 16000 \end{cases}$ $f = \begin{cases} 1.2575 + \frac{188.75}{Re}, & 90 < Re < 400 \\ 6.7Re^{-0.209}, & 400 < Re < 16000 \end{cases}$
Martin [21] (G)				$0-80$			$\frac{2b}{\phi}$						$\frac{1}{\sqrt{f}} = \frac{\cos\beta}{\sqrt{b\tan\beta + c\sin\beta + f_0/\cos\beta}} + \frac{1-\cos\beta}{\sqrt{a.f_{1,0}}}$ where $(a,b,c) = 3.8, 0.18, 0.36$ $f_0 = \frac{64}{Re}$ for Re < 2000 $f_{1,0} = \frac{597}{Re} + 3.85$ for Re < 2000
Bond [22] (G)			1.14	25- 60			$\frac{2b}{\phi}$						For $\beta =$ 60° $Nu = 0.309Re^{0.68}Pr^{1/3}\left(\frac{\mu}{\mu_w}\right)^{0.16}$ $f = \frac{3.1}{Re^{0.19}}$
Huang et al. [23] (G)	516	188	1.14	28/28 28/60 60/60	2	8.1	$\frac{2b}{\phi}$	22	12	11	A_p	Water	$100 \le Re \le 10000$ For 60/60° $Nu = 0.759Re^{0.53}Pr^{0.33}\left(\frac{\mu}{\mu_w}\right)^{0.17}$ $f = \frac{12.28}{Re^{0.161}}$
Yang et al. [24](B)	466 466 466 269 269	111 111 111 111 95	1.16 1.16 1.16 1.16 1.18	65 65 46.5 27 65	2 2 2 2 1.25	7 7 7 7 4	2b	10				Ethylene glycol/ Water mixture	Plate 1: $Nu = 0.341$ Plate 2: $Nu = 0.340$ Plate 3: $Nu = 0.164$ Plate 4: $Nu = 0.355$ Plate 5: $Nu = 0.248$

Chisholm and Wanniarachchi [25] (G)	172	95	1.18	65	1.25	4
	172	77	1.16	65	2	7
	172	77	1.16	46.5	2	7
		77	1.16	27	2	7
				30 − 80		

Plate 6: $Nu = 0.274$

Plate 7: $Nu = 0.341$

Plate 8: $Nu = 0.214$

Plate 9: $Nu = 0.155\left(\frac{90-\beta}{30}\right)^{0.66}\phi^{0.41}Re^{0.59}Pr^{0.4}$

$Nu_w = 0.724\left(\frac{90-\beta}{30}\right)\phi^{1.25}[(90-\beta)/30]^{3.6}$

$f = 0.80Re^{-0.25}\phi^{1.25}[(90-\beta)/30]^{3.6}$

$1000 \leq \mathrm{Re} \leq 40000,\ \mathrm{Pr} = 5$

Appendix B

The modification procedure is conducted through the following procedure

$$R_{tt} = \frac{A_{eff}\Delta T_{ln}}{Q} \tag{B1}$$

$$R_{tt} = \frac{\phi A_p \Delta T_{ln}}{Q} \tag{B2}$$

where $\frac{1}{U} = R_{tt}$

Eq. (B2) can be written as:

$$\frac{R_{tt}}{\phi} = \frac{A_p \Delta T_{ln}}{Q} \tag{B3}$$

The thermal resistance of wall conduction can be ignored as the convective thermal resistance is two or three orders of magnitude larger and thus Eq. (B3) can be written as:

$$\frac{R_{tt}}{\phi} = \frac{D_h}{\phi k_h C_1 {Re_h}^{C_2} {Pr_h}^{0.33}} + \frac{D_h}{\phi k_c C_1 {Re_c}^{C_2} {Pr_c}^{0.33}} \tag{B4}$$

Therefore, correlations that use A_{eff} as the heat transfer area can easily be modified into correlations that use A_p by multiplying the coefficient C_1 with the enlargement factor ϕ. The hydraulic diameter can be adjusted using a similar procedure where:

$$R = \frac{D_h}{k.\ C_1\left(\frac{GD_h}{\mu}\right)^{C_2} Pr^{0.33}} \tag{B5}$$

$$R = \frac{{}^{2b}/_{\phi}}{k.\ C_1\left(\frac{G\times 2b}{\phi\mu}\right)^{C_2} Pr^{0.33}} \tag{B6}$$

$$R = \frac{2b}{k.\ \phi^{1-C_2}.C_1\left(\frac{G\times 2b}{\mu}\right)^{C_2} Pr^{0.33}} \tag{B7}$$

where R is the convective heat transfer thermal resistance for either hot-side or cold-side of the heat exchanger. Therefore, correlations that take ${}^{2b}/_{\phi}$ as the hydraulic diameter can be simplified by multiplying C_1 by the coefficient ϕ^{1-C_2}.